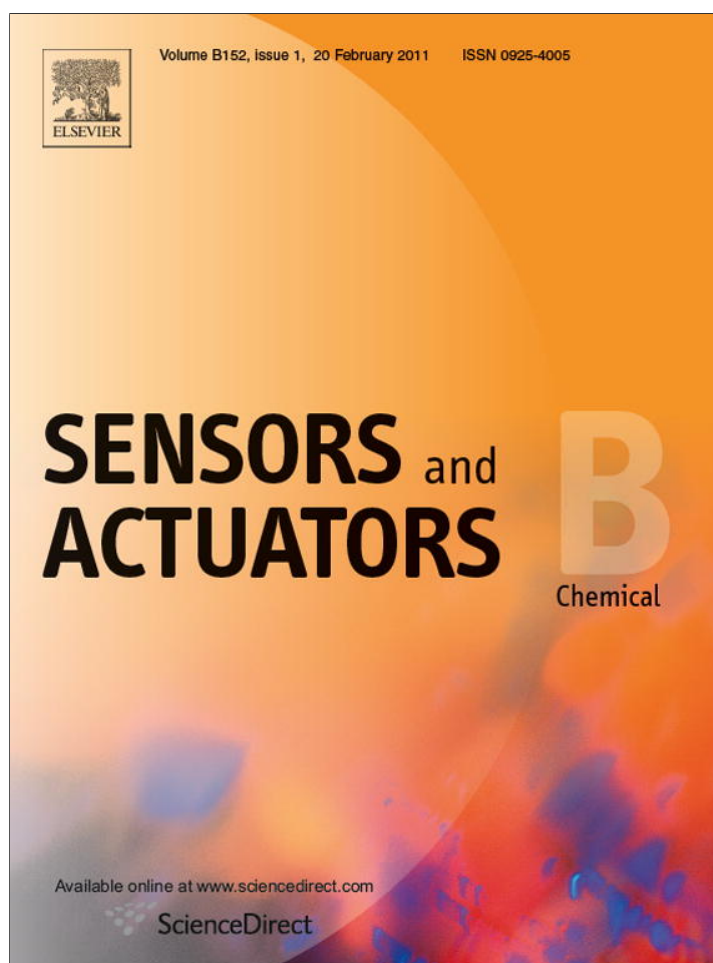


Provided for non-commercial research and education use.
Not for reproduction, distribution or commercial use.



This article appeared in a journal published by Elsevier. The attached copy is furnished to the author for internal non-commercial research and education use, including for instruction at the authors institution and sharing with colleagues.

Other uses, including reproduction and distribution, or selling or licensing copies, or posting to personal, institutional or third party websites are prohibited.

In most cases authors are permitted to post their version of the article (e.g. in Word or Tex form) to their personal website or institutional repository. Authors requiring further information regarding Elsevier's archiving and manuscript policies are encouraged to visit:

<http://www.elsevier.com/copyright>



Contents lists available at ScienceDirect

Sensors and Actuators B: Chemical

journal homepage: www.elsevier.com/locate/snb

Metal-enhanced fluorescence based calcium detection: Greater than 100-fold increase in signal/noise using Fluo-3 or Fluo-4 and silver nanostructures

Nina Bondre^a, Yongxia Zhang^a, Chris D. Geddes^{b,*}^a Institute of Fluorescence, University of Maryland Baltimore County, 701 East Pratt St, Baltimore, MD 21202, USA^b Institute of Fluorescence and Department of Chemistry and Biochemistry, University of Maryland Baltimore County, 701 East Pratt Street, Baltimore, MD 21202, USA

ARTICLE INFO

Article history:

Received 9 July 2010

Received in revised form 7 September 2010

Accepted 19 September 2010

Available online 8 October 2010

Keywords:

Metal-enhanced fluorescence

Fluo-3 and Fluo-4

Silver island films

ABSTRACT

In this paper we describe metal-enhanced fluorescence (MEF) of the Ca^{2+} indicators: Fluo-3 and Fluo-4 in close proximity to silver nano-particles, SiFs. When the concentration of Ca^{2+} increases, the MEF enhancement factor decreases, which is consistent with our previous findings that the greatest fluorescence enhancements occur for fluorophores with the lowest free-space quantum yield. Over 100-fold enhanced fluorescence intensities (signal/noise) were observed. In addition, the photostability of the fluorophore (Fluo-3) is much more prolonged from the SiFs as compared to glass (a control sample). Our findings strongly suggest the widespread use and the general approach of nanoparticulate SiFs surfaces for the enhanced detection of both intra and extra-cellular calcium and indeed other analytes of interest.

© 2010 Elsevier B.V. All rights reserved.

1. Introduction

Ca^{2+} functions as a ubiquitous intracellular messenger regulating many different cellular processes including fertilization, proliferation, secretion, metabolism, contraction and apoptosis [1,2]. The ability to measure Ca^{2+} concentration and signal Ca^{2+} pathways is of importance to build powerful tools for biotechnology settings and in the diagnosis of many diseases, such as hypoparathyroidism, tumor metastasis and renal failure [3,4]. There are many sensing schemes for calcium detection, such as lipophilic pH-sensitive indicator dyes based on the ion-exchange between the measured ion and a proton, or interaction of potential Ca^{2+} -sensitive dyes with a neutral ion carrier [3,5,6]. Many of those methods suffer from inherent pH-dependencies and instabilities associated with the leaching of critical components in intracellular studies.

About thirty years ago the design of fluorescent Ca^{2+} indicators, such as Quin-2 by Roger Tsien, enabled the first quantitative measurements of Ca^{2+} concentrations inside cells [7]. Today, dozens of different fluorescent probes have been created based on this approach [8]. These fluorescent indicators have been used to detect Ca^{2+} signals and to map the molecular mechanisms that are underlying cellular Ca^{2+} using microscopy. Although Quin-2 has revealed much important biological information, it has severe and acknowl-

edged limitations [8]: UV range excitation (339 nm), which could damage tissue/living cells as well as a shallow penetration depth, and very low free-space quantum yield (0.03).

In this regard, Fluo-3 and Fluo-4, which are the derivatives of 1,2-bis-(2-aminophenoxyethane) N,N,N',N'-tetraacetic acid, are today among the most widely used Ca^{2+} indicators because of their longer wavelength excitation, which invariably alleviates biological autofluorescence [9]. However, the detection limit is still underpinned by the quantum yield of the fluorophore (Fluo-3/Fluo-4), the autofluorescence of the sample and the photostability of the fluorophores, classical constraints of fluorophores, when used in the far-field condition.

In this regard, metallic nanostructures have been used to favorably modify the spectral properties of fluorophores and to alleviate some of their more classical photophysical constraints, such as increasing system quantum yield and decreased lifetimes, which leads to an increased photostability and fluorophore cyclic rate. The use of fluorophore-metal interactions has been termed metal-enhanced fluorescence (MEF) by Geddes and co-workers [10], whereby large fluorescence enhancements can be obtained from fluorophores that are in the near-field vicinity of metal nanoparticles. Owing to these advantages, there has been a significant interest in the uses of metal enhanced fluorescence. Many applications of metal-enhanced fluorescence (MEF) have been demonstrated [11–13], which have included improved DNA [14] and protein detection [15], the release of self-quenched fluorescence of over labeled proteins [16], enhanced wavelength-ratiometric sensing [17] and ultra fast and ultra sensitive target analyte detection [18], to name but just a few.

Abbreviations: MEF, metal-enhanced fluorescence; SiFs, silver island films.

* Corresponding author.

E-mail address: geddes@umbc.edu (C.D. Geddes).

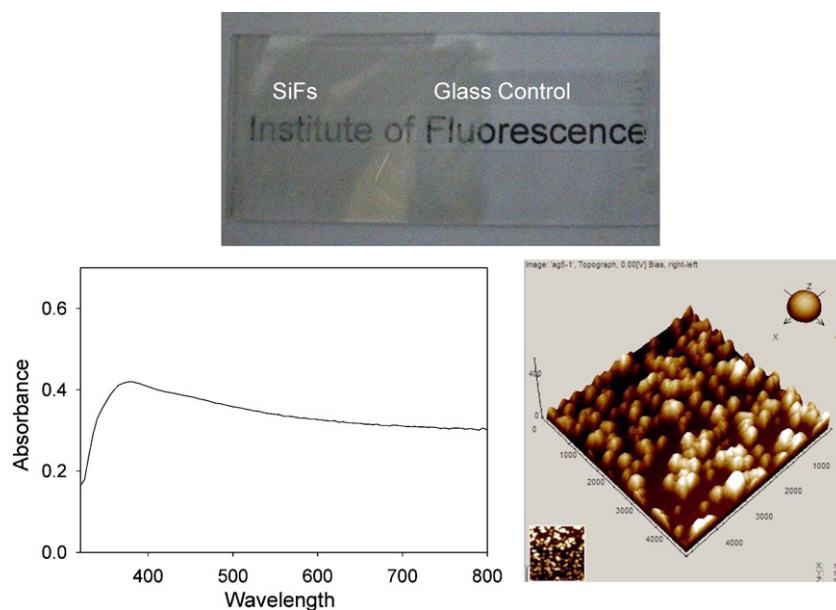


Fig. 1. Photograph of 90-s preparation time SiFs (top) and the respective plasmon absorbance spectrum of the 90-s SiFs and AFM (bottom).

In this paper, we have studied metal-enhanced fluorescence of the Ca^{2+} indicators: Fluo-3 and Fluo-4 in proximity to silver nanoparticles. We observed that Fluo-3 and Fluo-4 in the presence of silver nanoparticles without Ca^{2+} binding, enhances the far-field fluorescence about 400-fold and becomes dramatically more photostable. The enhancement factor was determined as the ratio of the fluorescence intensity from the silver island films as compared to a glass control surface, where no near-field Plasmon enhancement is observed. Our approach of using silver nanoparticles to enhance analyte indicator luminescence is of significant benefit to workers wishing to quantify lower levels of biological calcium and the detection scheme is also likely applicable to other sensing schemes and other analytes of interest as well.

2. Experimental

2.1. Materials

Silver nitrate (99.9%), sodium hydroxide (99.996%), ammonium hydroxide (30%), D-glucose and premium quality silane-prep glass slides (75 mm \times 25 mm) were purchased from Sigma–Aldrich. The calcium calibration buffer kit with 11 calcium concentrations ranging from 0 to 39 μM (0, 0.017, 0.038, 0.065, 0.100, 0.150, 0.225, 0.351, 0.602, 1.35, and 39 μM), Fluo-3 (pentaammonium salt, MW = 854.7 g) and Fluo-4 (pentapotassium salt, MW = 1055.26 g) were purchased from Invitrogen. All chemicals were used as received.

2.2. Preparation of silver island films (SiFs)

Silver island films were prepared in accordance with previously established procedures [19]. In said procedures, D-glucose is used to reduce silver nitrate to form silver islands on one surface of the glass slide. The thickness of the SiFs and indeed nanoparticle size can be varied depending on the length of time silver is allowed to deposit on the slides [20]. The SiFs used for MEF of Fluo-3 and Fluo-4 in this study had a deposition time of 90 s. The SiFs were characterized by their absorbance spectrum and atomic force microscopy (AFM) images as shown in Fig. 2. A photograph of the SiFs is also shown in Fig. 1.

2.3. Preparation of the sandwich format sample

1 mg of Fluo-3 was dissolved in 500 μL of water to form a 2.34 mM stock solution, and 500 μg of Fluo-4 were dissolved in 500 μL of water to form a 948 μM stock solution. 2 μL of Fluo-3 in water was trapped in a sandwich format along with calcium buffer between the glass slides and the silver island films, respectively. The final concentration of the indicator probe was 47 μM . For Fluo-4, 3 μL of dye in water was used, for a final concentration of 28 μM .

2.4. Absorption and fluorescence measurements

To measure the absorbance and emission spectra of Fluo-3 in solution, 3 μL of stock solution was added to 1 mL of each of the concentrations of calcium buffers in a quartz cuvette. The final concentration of Fluo-3 was 7 μM . A similar procedure was followed to obtain the emission spectra of Fluo-4, except that a final concentration of 6 μM was obtained. Absorbance spectra were taken using a Varian Cary 50 UV–Vis Spectrophotometer. Fluorescence spectra were collected with a Varian Eclipse spectrofluorometer with an excitation of 473 nm.

2.5. Emission of Fluo-3 and Fluo-4 on SiFs and glass slides

A 100 μL solution of Fluo-3 and 1 of 11 calcium concentration buffers was sandwiched between two glass slides and then SiFs with a glass slide on top, to measure the fluorescence emission. The same SiFs slide was washed between samples with de-ionized water and then dried with nitrogen gas. Samples were excited using a 473 nm laser, and emission spectra were collected with an Ocean Optics HR2000 Fluorometer and a RazorEdge™ 473 nm filter. An integration time of 300 ms was kept constant for all measurements. The intensity at 526 nm for each calcium concentration was fitted to a power function. Similarly, for Fluo-4, the intensity at 518 nm for each calcium concentration was collected and also fitted to a power function.

2.6. Fluorescence lifetime measurements and analysis

Lifetime measurements for Fluo-3 were undertaken using a TemPro Fluorescence Lifetime System (Horiba Jobin Yvon), with

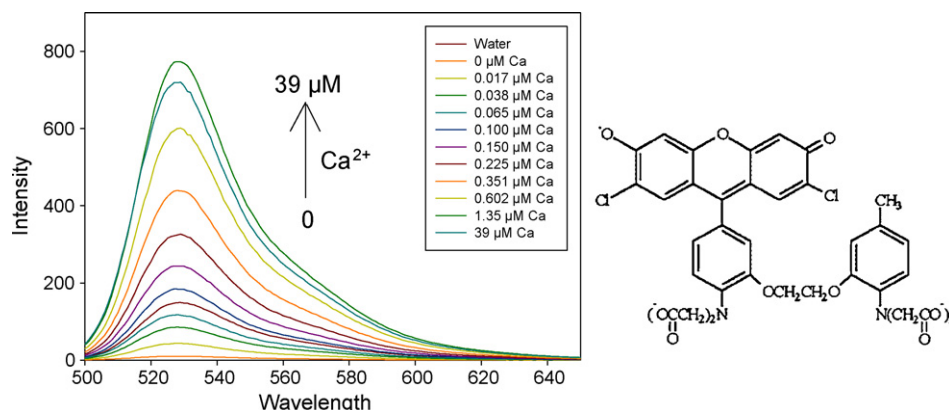


Fig. 2. Emission spectra of 7 μM Fluo-3 in 1 mL of CaEGTA, $[\text{Ca}^{2+}]$ ranging from 0 to 39 μM , with samples excited at 473 nm in a quartz cuvette (left). Molecular structure of Fluo-3 (right).

samples excited at 454 nm. The lifetime of Fluo-3 in 39 μM calcium buffer was measured in a quartz cuvette, with the probe's final concentration being 21 μM . A sandwich of glass slides and one sandwich of SiFs and a glass slide were then measured, with 100 μL of the described solution trapped between the slides. Biexponential models were fitted to the data utilizing DAS6 software (Horiba Jobin Yvon).

The intensity decays were analyzed in terms of the multi-exponential model:

$$I(t) = \sum_i \alpha_i \exp\left(\frac{-t}{\tau_i}\right) \quad (1)$$

where α_i are the amplitudes and τ_i are the decay times, $\sum_i \alpha_i = 1.0$.

The fractional contribution of each component to the steady state intensity is given by

$$f_i = \frac{\alpha_i \tau_i}{\sum_j \alpha_j \tau_j} \quad (2)$$

The mean lifetime of the excited state is given by

$$\bar{\tau} = \sum_i f_i \tau_i \quad (3)$$

and the amplitude-weighted lifetime is given by

$$\langle \tau \rangle = \sum_i \alpha_i \tau_i \quad (4)$$

The values of α_i and τ_i were determined by a nonlinear least squares impulse reconvolution analysis with a goodness-of-fit χ^2 criterion.

2.7. Photostability

The steady-state fluorescence intensity decay of Fluo-3 was measured using the sandwich format with an Ocean Optics HR2000 Fluorometer and a RazorEdge™ 473 nm filter. Glass slides functioned as a control sample by which to compare with a SiFs sandwich, with the probe in 39 μM calcium buffer. The initial intensity on SiFs was adjusted to that observed on glass using a 0.40 neutral density filter (Edmund Optics) in order to compare fluorescence intensity decays. The final concentration of Fluo-3 was 178 μM . The photon flux yield was also calculated, comparing that from SiFs with that observed from glass.

3. Results and discussion

Fluo-3 is synthesized from 1,2-bis-(2-aminophenoxyethane) N,N,N',N' -tetraacetic acid (BAPTA) by combination with a fluorescein-like structure (Fig. 2 right) [7,9]. Emission spectra of Fluo-3 in solution when excited at 473 nm are shown in Fig. 2. It was observed that there is no bathochromic shift after Ca^{2+} binding with Fluo-3, the fluorescence increasing with $[\text{Ca}^{2+}]$ from 0 to 39 μM . Tsien and co-workers explained the lack of shift of the dye, as due to the severe steric hindrance between the rigidly planar xanthene chromophore and the benzene ring of the BAPTA [7], where these dyes are typically shown to have blue or red shifts upon electron donation and withdrawal from the corresponding position on the chromophores backbone. Tsien also reported how the Ca^{2+} binding increases the quantum efficiency, and explained how it is due to a significant resonance formation which increases bond orders from the amino nitrogen to the benzene ring and subsequently to the xanthene chromophore. Such an increased double-bond character results in less nonradiative deactivation from the excited state, and hence higher free-space quantum yields and lifetimes are observed.

When the fluorophores are in close proximity to silver nanoparticles in the SiFs film geometry, the fluorescence emission intensities of Fluo-3 can be increased dramatically. From Fig. 3, the fluorescence enhancement factor was over 400-fold in solution without any Ca^{2+} binding, as compared to the control sample on glass/glass. The real color photograph (Fig. 3 top) also shows that the emission intensity is much more clearly detectable from the SiFs/glass as compared to the glass/glass control sample wells. With the concentration of Ca^{2+} increasing, the enhancement factor is decreased. Our laboratories mechanistic interpretation of MEF is underpinned by a model whereby non-radiative energy transfer occurs from excited distal fluorophores to surface plasmons in non-continuous films, in essence a fluorophore induced mirror dipole in the metal. The surface plasmons, *in turn*, radiate the photophysical characteristics of the coupling fluorophores. In essence, the system radiates as a whole. As a result, the system exhibits modified overall radiative rates, in contrast to the fluorophore itself whose rate is thought unchanged. Ultimately, the increased radiative rate for the system lends to enhanced fluorescence signals for fluorophores in close proximity to metallic structures. The important factors which could affect the magnitude of the fluorescence enhancement via the localized surface plasmon resonance (LSPR) are the size and shape of the nanoparticles, the degree of overlap between the LSPR and the emission band of the dye, as well as the far-field free-space value of the quantum yield. The greatest enhancements are typically observed for fluorophores with the lowest free space

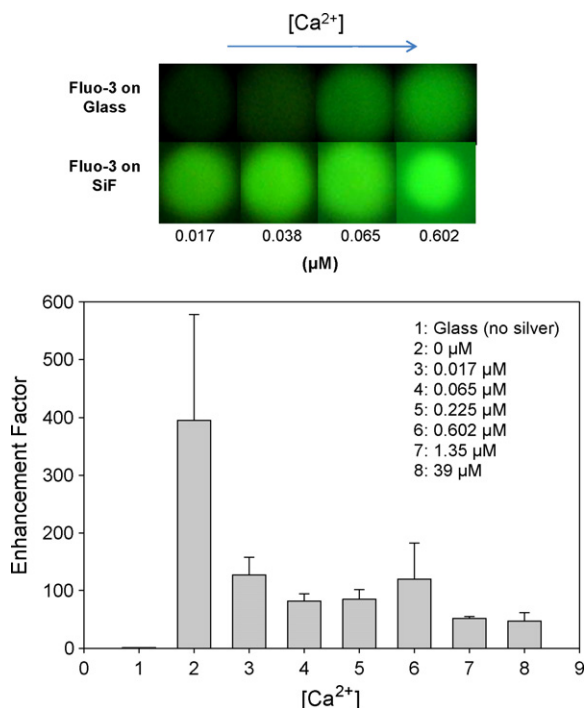


Fig. 3. Fluorescence enhancement factor for 47 μM Fluo-3 in CaEGTA.

quantum yield, which we also observed here (Fig. 3). The shape and full width at half maximum of Fluo-3 spectra on glass and SiFs were also compared. Fig. 4 shows the full width at half maximum (FWHM) for the fluorescence spectral data for Fluo-3 in different Ca²⁺ concentration solution on glass and on SiFs, where the FWHM on SiFs are very similar to that of the spectra measured on glass bottomed wells, demonstrating the mirrored quanta in the MEF effect.

We have summarized the fluorescence intensity of Fluo-3 with various [Ca²⁺] from glass/glass and glass/SiFs wells, respectively in Fig. 5. Fig. 5 top shows the comparison of the intensity of Fluo-3 emission at 526 nm in Ca²⁺ from 0.017 to 1.35 μM on SiFs and glass slides. In Fig. 5 bottom, we show the log intensity vs. log Ca concentration, which shows a linear relation which can be used as calibration plot to measure [Ca²⁺]. From the plots, we can see the detection limit is significantly extended when using SiFs as compared to glass. Most notably, the overall emission intensity on SiFs

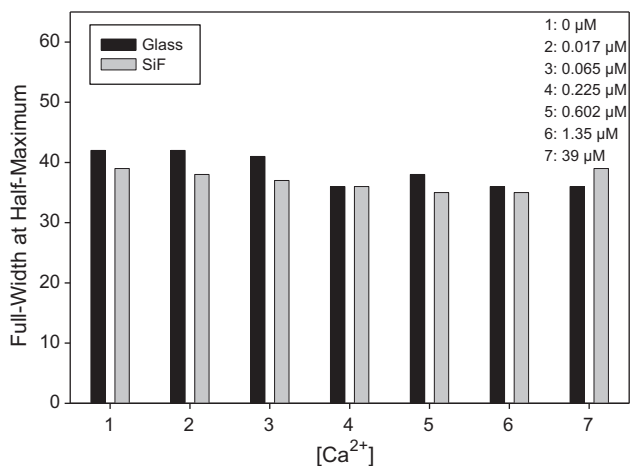


Fig. 4. Comparison of full-width at half-maximum (FWHM) for 47 μM Fluo-3 in CaEGTA on SiFs and glass slides, samples excited at 473 nm.

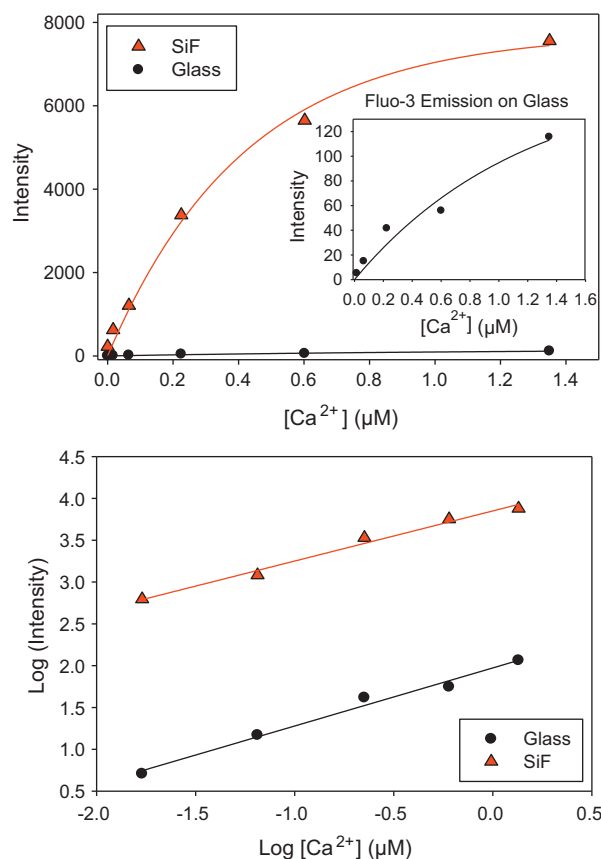


Fig. 5. Comparison of the intensity of Fluo-3 emission at 526 nm in CaEGTA, [Ca²⁺] ranging from 0.017 to 1.35 μM on SiFs and glass slides, a control sample. Plot of intensity vs. [Ca²⁺] (top) and plot of log (intensity) vs. Log [Ca²⁺] (bottom).

is 2log₁₀ higher and most importantly, the response curve to [Ca²⁺] remains the same linear function on SiFs as compared to glass.

Almost all fluorophores are photobleached with continuous light illumination. Photobleaching is a ubiquitous problem in the application of fluorescence. In this regard, the photostability of Fluo-3 on SiFs and glass was also studied. Fig. 6 shows Fluo-3 emission as a function of time, excited at 473 nm and observed through a 473 nm razor edge filter. The relative intensities of the plots reflect that more detectable photons can be observed per unit time from the SiFs film, as compared to glass (a control sample), where the integrated areas under the plots are proportional to the

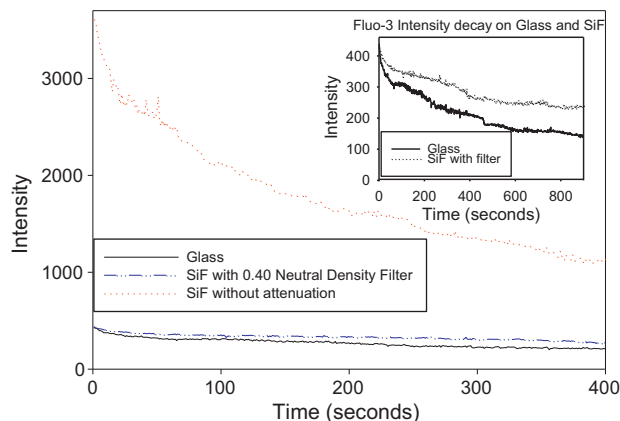


Fig. 6. Fluorescence intensity decay for 187 μM Fluo-3 in CaEGTA on glass slides and 90-s SiFs also, using a 0.40 neutral density filter on SiFs to adjust the original intensity to match that observed on glass.

Table 1
Fluo-3 lifetime analysis in 39 μM Ca^{2+} on glass and on SiFs, measured using time-domain fluorometry. τ mean lifetime, $\langle\tau\rangle$ -amplitude-weighted lifetime. Excitation: 454 nm. The lifetime on SiFs was too short to be measured.

	T_1 (ns)	A_1 (%)	T_2 (ns)	A_2 (%)	$\langle\tau\rangle$ (ns)	$\bar{\tau}$ (ns)	χ^2
Fluo-3 in 39 μM Ca^{2+} in a cuvette	0.79	94.03	2.67	5.97	0.74	0.78	1.50
On glass/glass	0.54	30	0.89	70	0.78	0.81	1.33
On SiFs/glass	–	–	–	–	<0.2	<0.2	–

photon flux from the respective samples. By additionally adjusting the laser power to match the same initial steady-state intensities of the samples, the Fluo-3 on SiFs can be seen to be more photostable compared with that on glass/glass. This finding suggests that the lifetime on the SiFs is also shorter than on the glass film, the Fluo-3 in essence spending less time on average in an excited state due to the fast non-radiative energy transfer to the SiFs and therefore is less prone to photo destruction, i.e. is more photostable.

In this regard, we have also measured the time-resolved intensity decays of Fluo-3 in 39 μM Ca^{2+} (fluorescence lifetimes) in close proximity to SiFs, data shown in Table 1. The respective lifetimes were calculated from those decays, using non-linear least squares impulse reconvolution analysis. We see both a reduced amplitude-weighted lifetime ($\langle\tau\rangle$ on SiFs <0.2 ns) and mean lifetime (τ_{mean} on SiFs <0.2 ns) as compared to the glass control sample (τ_{mean} on glass = 0.81 ns and $\langle\tau\rangle$ on glass = 0.78 ns), which also supports the enhanced observed photostabilities.

Finally, we have also studied Fluo-4 in proximity to silver nanoparticles. It shows very similar metal-enhanced fluorescence characteristics as Fluo-3. The fluorescence spectra and real color photographs are shown in Fig. 7, where very similar photophysics was observed for Fluo-3 and -4 near-to the SiFs.

3.1. Enhancement factor trend

For fluorophores in the far-field condition (i.e. greater than 1 wavelength away from any surface support or structure), the fluorescence quantum yield and lifetime are described by the familiar rate equations:

$$Q_0 = \frac{\Gamma}{\Gamma + k_{\text{nr}}} \quad (5)$$

$$\tau_0 = \frac{1}{\Gamma + k_{\text{nr}}} \quad (6)$$

where Γ is the far-field fluorophore radiative rate, k_{nr} are the none radiative rates, Q_0 the quantum yield and τ_0 is the free-space fluorophore lifetime.

For Fluo-3 in the presence of calcium in the far-field condition (i.e. glass bottomed wells), we see that both the lifetime and quantum yield change in unison, i.e. both proportionately increase with increased calcium (Fig. 2).

However, for fluorophores in the near-field condition close-to metallic nanoparticles (i.e. SiFs bottomed wells), one typically observes an increased system quantum yield, Q_m , coupled with a decreased system lifetime, τ_m , described by the following

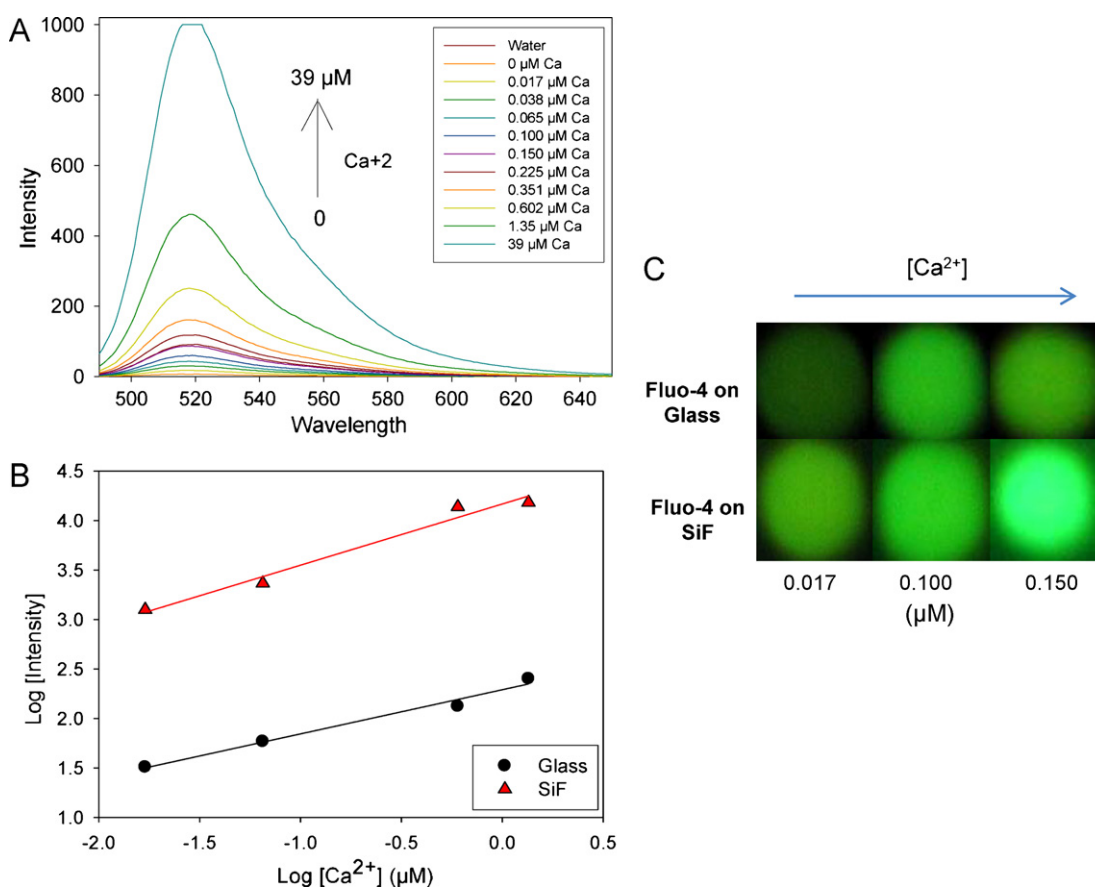


Fig. 7. (A) Emission spectra of 6 μM Fluo-4 in 1 mL of CaEGTA, $[\text{Ca}^{2+}]$ ranging from 0 to 39 μM , with samples excited at 473 nm in a cuvette. (B) Plot of log (intensity) vs. log $[\text{Ca}^{2+}]$ (μM). (C) Real-color photographs of Fluo-4 on glass slides and SiFs, visually demonstrating the enhanced fluorescence observed from the SiFs surface.

fluorophore-metallic particle system rate equations:

$$Q_m = \frac{\Gamma + \Gamma_m}{\Gamma + \Gamma_m + k_{nr}} \quad (7)$$

$$\tau_m = \frac{1}{\Gamma + \Gamma_m + k_{nr}} \quad (8)$$

where τ_m , Q_m and Γ_m are the metal-modified system lifetimes, quantum yield and radiative rate, respectively. From Eqs. (7) and (8), we can readily see that as the coupled system radiative rate increases, the quantum yield increases, while the lifetime subsequently drops, a notable change from the fluorescence far-field condition.

Subsequently, for Fluo-3 near-to SiFs, the greatest enhancement factors are obtained for the lowest calcium concentrations (Fig. 3), i.e. where the free-space quantum yield is the lowest, consistent with Eqs. (7) and (8). Similarly, for fluorophores near-to the metal, the system radiative lifetime is reduced, a fluorophore therefore spending less time on average in an excited state prior to its return to the ground state, and is thus statistically more photostable (Fig. 6). In terms of overall sensing and the detectability of calcium concentrations, the increased photostability lends to a greater photon flux (more photons per unit time) and when accompanied by an increased net system quantum yield leads to a substantial overall increase in calcium detectability (greater than 100-fold). A detailed description of the wavelength dependence of the MEF effect, which outlines the enhancement mechanism in more detail can be found in a recent report by us [21].

4. Conclusions

For the fluorophores (Fluo-3 and Fluo-4) in close proximity to silver nanoparticles, the fluorescence emission intensities can be increased dramatically. For Fluo-3, the fluorescence enhancement factor was over 100-fold in solution with $0.017 \mu\text{M}$ Ca^{2+} as compared with the control sample on glass/glass. With the concentration of Ca^{2+} increasing, the enhancement factor decreased (total brightness increased) which is consistent with our previously observed trends that the greatest enhancements are observed for the fluorophores with the lowest free-space quantum yield. The photostability of the Fluorophore (Fluo-3) is significantly improved on the SiFs film as compared to glass (a control sample). In addition, a shorter metal-modified lifetime of Fluo-3 was also observed, which supports the trend in the enhanced photostability. Given the widespread use of both Fluo-3 and Fluo-4 for calcium detection, then our findings suggest that SiFs surfaces can be employed for the enhanced S/N detection of $[\text{Ca}^{2+}]$ in biological applications, particularly in 96-well formats and for coated glass microscope slides. Further, the SiFs surfaces and the use of low free-space quantum yield fluorophores in the indicator-unbound form, is likely to be a general approach for the MEF sensing of other analytes as well. Further studies are underway and will be reported by our laboratory in due course.

Acknowledgements

The authors would like to thank the IoF (Institute of Fluorescence), Department of Chemistry and Biochemistry and the University of Maryland Baltimore County for salary support.

References

- [1] B.J. Michael, B.D. Martin, L. Peter, Calcium—a life and death signal, *Nature* 395 (1998) 645–648.
- [2] M.J. Berridge, Neuronal calcium signaling, *Neuron* 21 (1) (1998) 13–26.
- [3] A. Takahashi, P. Camacho, J.D. Lechleiter, B. Herman, Measurement of intracellular calcium, *Physiological Reviews* 79 (4) (1999) 1089–1125.

- [4] H. He, K. Jenkins, C. Lin, A fluorescent chemosensor for calcium with excellent storage stability in water, *Analytica Chimica Acta* 611 (2008) 197–204.
- [5] O.S. Wolfbeis, B.P.H. Schaffara, Optical sensors: an ion-selective optode for potassium, *Analytica Chimica Acta* 198 (1987) 1–7.
- [6] W.E. Morf, K. Seiler, B. Rusterholz, W. Simon, Design of a novel calcium-selective optode membrane based on neutral ionophores, *Analytical Chemistry* 62 (1990) 738–742.
- [7] A. Minta, J.P.Y. Kao, R. Tsien, Fluorescent indicators for cytosolic calcium based on rhodamine and fluorescein chromophores, *The Journal of Biological Chemistry* 264 (14) (1989) 8171–8178.
- [8] G. Grzegorz, P. Martin, T.Y. Roger, A new generation of Ca^{2+} indicators with greatly improved fluorescence properties, *The Journal of Biological Chemistry* 260 (6) (1985) 3440–3450.
- [9] G. Grynkiewicz, M. Poenie, R.Y. Tsien, A new generation of Ca^{2+} indicators with greatly improved fluorescence properties, *The Journal of Biological Chemistry* 260 (6) (1985) 3440–3450.
- [10] C.D. Geddes, J.R. Lakowicz, Metal-enhanced fluorescence, *Journal of Fluorescence* 12 (2) (2002) 121–129.
- [11] C.D. Geddes, A. Parfenov, I. Gryczynski, J. Malicka, D. Roll, J.R. Lakowicz, Fractal silver structures for metal-enhanced fluorescence: applications for ultra-bright surface assays and lab-on-a-chip-based nanotechnologies, *Journal of Fluorescence* 13 (2) (2003) 119–122.
- [12] C. Guarise, L. Pasquato, V. De Filippis, P. Scrimin, Gold nanoparticles-based protease assay, *Proceedings of the National Academy of Sciences of the United States of America* 103 (11) (2006) 3978–3982.
- [13] C.Z. Li, K.B. Male, S. Hrapovic, J.H. Luong, Fluorescence properties of gold nanorods and their application for DNA biosensing, *Chemical Communications (Camb)* 31 (2005) 3924–3926.
- [14] K. Aslan, S.N. Malyn, C.D. Geddes, Fast and sensitive DNA hybridization assays using microwave-accelerated metal-enhanced fluorescence, *Biochemical and Biophysical Research Communications* 348 (2) (2006) 612–617.
- [15] K. Aslan, I. Gryczynski, J. Malicka, E. Matveeva, J.R. Lakowicz, C.D. Geddes, Metal-enhanced fluorescence: an emerging tool in biotechnology, *Current Opinion in Biotechnology* 16 (1) (2005) 55–62.
- [16] K. Aslan, V.H. Perez-Luna, Quenched emission of fluorescence by ligand functionalized gold nanoparticles, *Journal of Fluorescence* 14 (4) (2004) 401–405.
- [17] K. Aslan, J.R. Lakowicz, H. Szmajnski, C.D. Geddes, Enhanced ratiometric pH sensing using SNAFL-2 on silver island films: metal-enhanced fluorescence sensing, *Journal of Fluorescence* 15 (1) (2005) 37–40.
- [18] K. Aslan, C.D. Geddes, Microwave-accelerated metal-enhanced fluorescence: platform technology for ultrafast and ultrabright assays, *Analytical Chemistry* 77 (24) (2005) 8057–8067.
- [19] K. Aslan, Z. Leonenko, J.R. Lakowicz, C.D. Geddes, Annealed silver-island films for applications in metal-enhanced fluorescence: interpretation in terms of radiating plasmons, *Journal of Fluorescence* 15 (5) (2005) 643–654.
- [20] R. Pribik, A.I. Dragan, Y. Zhang, C. Gaydos, C.D. Geddes, Metal-enhanced fluorescence (MEF): physical characterization of silver island films and exploring sample geometries, *Chemical Physics Letters* 478 (2009) 70–74.
- [21] Y. Zhang, A. Dragan, C.D. Geddes, Wavelength-dependence of metal-enhanced fluorescence, *Journal of Physical Chemistry C* 113 (2009) 12095–12100.

Biographies

Nina Bondre is a sophomore at Duke University, majoring in Neuroscience and International Comparative Studies. She then plans to pursue a Masters in Prosthetics & Orthotics. This work is done during her internship in Institute of Fluorescence.

Dr. Yongxia Zhang is an Assistant Professor in Institute of Fluorescence, University of Maryland Baltimore County. Her research has been focusing on fundamental study of metal-enhanced fluorescence (MEF) and metal-enhanced phosphorescence (MEP) photophysical phenomenon, including design, development and characterization of advanced materials. At the fundamental level, it is hoped to elucidate, with molecular details, key factors, such as particle size, shape, crystal structure that influence the properties and functionalities of the nanomaterials interaction with fluorophore. In the meantime, Dr. Zhang's research is focused on Plasmonic Pumped Triplet States (PPTS) and their applications in microbiology and medicine. Dr. Zhang has published over 40 papers.

Dr. Chris D. Geddes, Ph.D., Professor, has extensive experience in fluorescence spectroscopy, particularly in fluorescence sensing and metal-fluorophore interactions (metal-enhanced fluorescence), publishing over 200 papers and 21 books. Dr. Geddes is internationally known in fluorescence for his scholarly publications and for the development of fluorescence-based plasmonics. He is the editor-in-chief of the *Journal of Fluorescence* and founding editor of the *Who's Who in Fluorescence* and *Annual Reviews in Fluorescence* volumes. In addition, due to the labs pioneering efforts in the fields of metallic nanoparticle-fluorophore interactions, Dr. Geddes launched the Springer Journal "Plasmonics" in 2005. Dr. Geddes is Director of the Institute of Fluorescence at the University of Maryland Baltimore County which focuses on the nano-bio-technological applications of fluorescence. Dr. Geddes frequently chairs NIH study sections, is a frequent member of the NIBIB special emphasis sensing panels and is currently a permanent member of the NIH EBT study section. Dr. Geddes currently has 24 patent families, housing over 75 individual world wide patents.